Measurements of the $\gamma\gamma^* \to \pi^0$ and $\gamma\gamma^* \to \eta_c$ transition form factors at BABAR

V. P. Druzhinin[1)]

Budker Institute of Nuclear Physics, Novosibirsk 630090, Russia

Abstract We present measurements of the $\gamma\gamma^* \to \pi^0$ transition form factor for the momentum transfer range Q^2=4–40 GeV^2 and the $\gamma\gamma^* \to \eta_c$ transition form factor for the range Q^2=2–50 GeV^2. The current status of measurements of the meson-photon transition form factors for the η and η' mesons is discussed. The results of the measurement of the η_c mass, total and two-photon widths are also presented.

Key words two-photon interaction, pseudoscalar meson, transition form factor, pi0, eta, eta(958), etac

PACS 12.38.Qk,13.40.Gp,13.60.Le

1 Introduction

The diagram for the process of the two-photon production of the pseudoscalar meson is shown in Fig. 1. The effect of strong interactions in this process is described only one form factor $F(q_1^2, q_2^2)$ depending on the squared momentum transfers to the electrons.

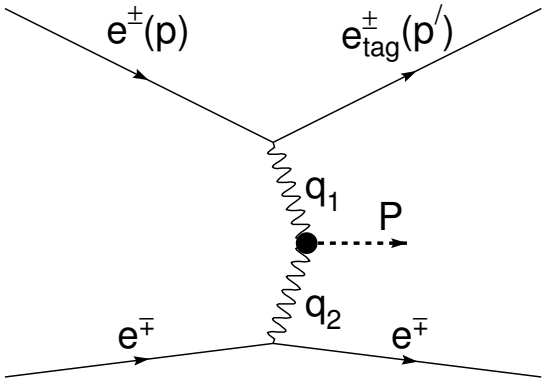

Fig. 1. The Feynman diagram for the process of the pseudoscalar meson two-photon production.

The electrons in such process are scattered predominantly at small angle. Therefore, the two-photon processes are usually studied in so called no-tag mode with both final electrons undetected. In this case the virtual photons are practically real, the momentum transfers squared are close to zero. In no-tag mode the meson-photon transition form factor at zero q^2's and the two-photon width of the meson are measured. In single tag-mode one of the final electron is detected. The corresponding virtual photon is highly off-shell. From the measurement of the cross section we extract more rich information: the dependence of the meson form factor on $Q^2 = -q_1^2$.

At large Q^2 perturbative QCD (pQCD) predicts that the transition form factor can be written as a convolution of a calculable hard scattering amplitude for $\gamma\gamma^* \to q\bar{q}$ with a nonperturbative meson distribution amplitude (DA), $\phi(x,Q^2)$ [1]. The latter can be interpreted as the amplitude for the transition of the meson with momentum p into two quarks with momenta px and $p(1-x)$. The experimental data on the transition form factor can be used to test different phenomenological models for the DA.

The cross section of the process $e^+e^- \to e^+e^-P$ falls very rapidly with increase of Q^2 (Q^{-6} for π^0). Therefore, a precise measurement of the transition form factor can be performed only at high luminosity e^+e^- machines. We present the results of the measurements of the transition form factors for π^0 and η_c mesons performed by the BABAR detector at the PEP-II e^+e^- collider. The results are based on data with integrated luminosity of about 450 fb^{-1} collected at the center-of-mass energy of 10.6 GeV. The single-tag events are selected with detected and identified

Received 26 January 2010

1) E-mail: druzhinin@inp.nsk.su

electron and with fully reconstructed π^0 or η_c. It is required that the transverse momentum of electron-plus-meson system be low and the missing mass in an event be close to zero.

We also discuss current experimental status on the meson-photon transition form factors for the η and η' mesons.

2 Measurement of the $\gamma^*\gamma \to \pi^0$ transition form factor [2]

The π^0 meson is detected via its decay into two photons. The two-photon invariant mass spectrum for selected π^0 candidates is shown in Fig. 2. The clear π^0 peak is seen. The main non-peaking background process is so called virtual Compton scattering (VCS), the precess $e^+e^- \to e^+e^-\gamma$ with one of the final electrons directed along the beam axis. The VCS photon together with a soft photon, for example from beam background, may give an invariant mass value close to the π^0 mass. The peaking background comes from the process of two-photon production of two π^0's. This background is estimated from data and is about 10% of signal events. The total number of signal events determined from the fit to the mass spectrum in Fig. 2 is about 13000. This number is an order of magnitude large than the statistics of the previous measurement of the form factor by CLEO [3].

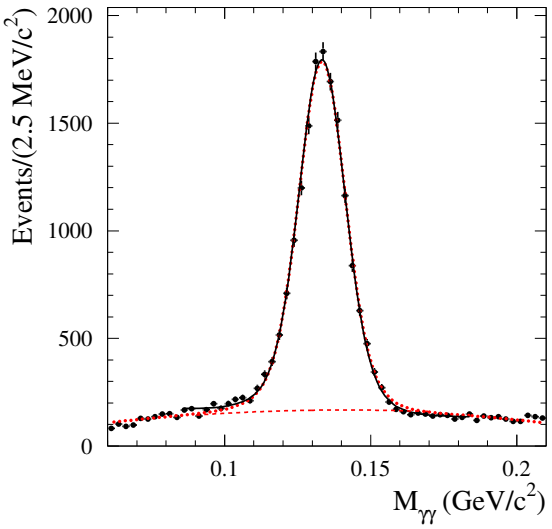

Fig. 2. The two-photon invariant mass spectrum for data events with $4 < Q^2 < 40$ GeV^2 and fitting curves.

We measure the form factor in the Q^2 region from 4 to 40 GeV^2. The lower Q^2 limit is determined by the detector acceptance for the electron. For $Q^2 > 40$ GeV^2 we do not see evidence of a π^0 signal over background. The data were divided into 17 Q^2 intervals. For each Q^2 interval the mass spectrum is fitted by a sum of signal and background distributions. From the measured Q^2 spectrum we determine the differential cross section for $e^+e^- \to e^+e^-\pi^0$ and the transition form factor. The result for the form factor is shown in Fig. 3. The errors shown are combined statistical and Q^2-dependent systematic. There is also Q^2-independent error equal to 2.3%. Main sources of the systematic uncertainties are background subtraction, data-MC simulation difference in the detector response, and the model uncertainty due to the unknown q_2^2 dependence of the form factor.

The comparison of our results with previous measurements [3, 4] is shown in Fig. 3. In the Q^2 range from 4 to 9 GeV^2 our results are in reasonable agreement with the measurements by the CLEO collaboration [3], but have significantly better precision.

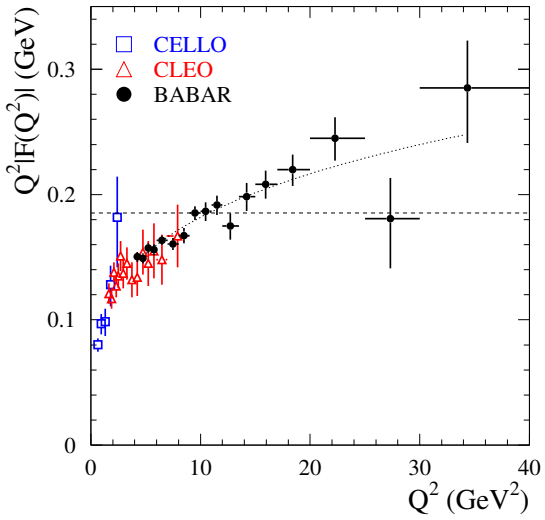

Fig. 3. The $\gamma\gamma^* \to \pi^0$ transition form factor multiplied by Q^2. The dashed line indicates the asymptotic limit for the form factor. The dotted curve shows the interpolation given by Eq. (2).

The horizontal dashed line indicates the asymptotic limit for the form factor. The value of the asymptotic limit

$$Q^2 F(Q^2) = \sqrt{2} f_\pi \approx 0.185 \ \text{GeV} \qquad (1)$$

is predicted by pQCD. The measured form factor exceeds the asymptotic limit at $Q^2 > 10$ GeV^2. This is an unexpected behavior; most models for the pion

DA give form factor approaching the limit from below (see, e.g., Ref. [5] and references therein). Our data in the range from 4 to 40 GeV^2 are well described by the function

$$Q^2|F(Q^2)| = A\left(\frac{Q^2}{10\ \text{GeV}^2}\right)^{\beta}, \qquad (2)$$

with $A = 0.182 \pm 0.002$ GeV and $\beta = 0.25 \pm 0.02$ (dotted line in Fig. 3). The effective Q^2 dependence of the measured form factor is $\sim 1/Q^{3/2}$.

Figure 4 demonstrates the comparison of our measurement with the result of the NLO QCD calculations performed by Bakulev, Mikhailov, and Stefanis [6] for the three models of the pion DA: asymptotic [7], Chernyak-Zhitnitsky (CZ) [8], and the DA derived from QCD sum rules with non-local condensates (BMS) [9]. There is a large difference between data and theory in Q^2 dependence. We conclude that all these models are inadequate for $Q^2 < 15$ GeV^2. For $Q^2 > 20$ GeV^2 the theoretical uncertainties are expected to be smaller. In this region our data lie above asymptotic limit and are consistent with CZ model. It should be noted that the CZ DA is widest of the three DA's discussed.

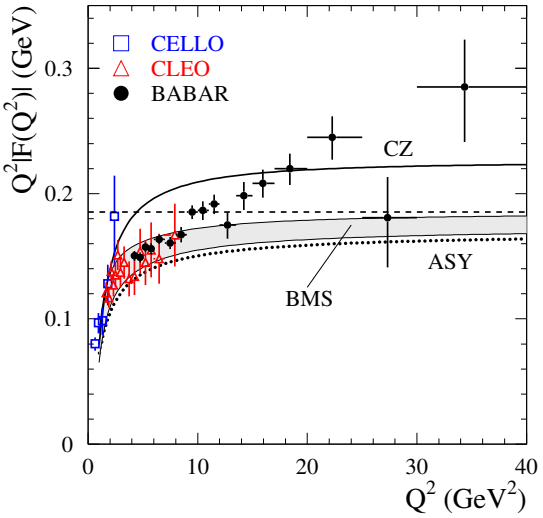

Fig. 4. The $\gamma\gamma^* \to \pi^0$ transition form factor multiplied by Q^2. The dashed line indicates the asymptotic limit for the form factor. The solid and dotted lines, and shaded band at the right panel show the predictions for the form factor for the CZ [8], asymptotic (ASY) [7], and BMS [9] models of the pion distribution amplitude, respectively.

There are theoretical works which appeared after the publication of our result. Mikhailov and Stefanis [10] argue that the growth of form factor cannot be explained by higher-order pQCD and power corrections. Other works [11–14] consider flat or very wide pion DA. With such distribution amplitude the Q^2 dependence observed by BABAR is reproduced well.

3 The $\gamma^*\gamma \to \eta$ and $\gamma^*\gamma \to \eta'$ transition form factors

The η and η' transition form factors were measured in the two-photon reactions $e^+e^- \to e^+e^-\eta^{(\prime)}$ in several experiments [3, 15–17].

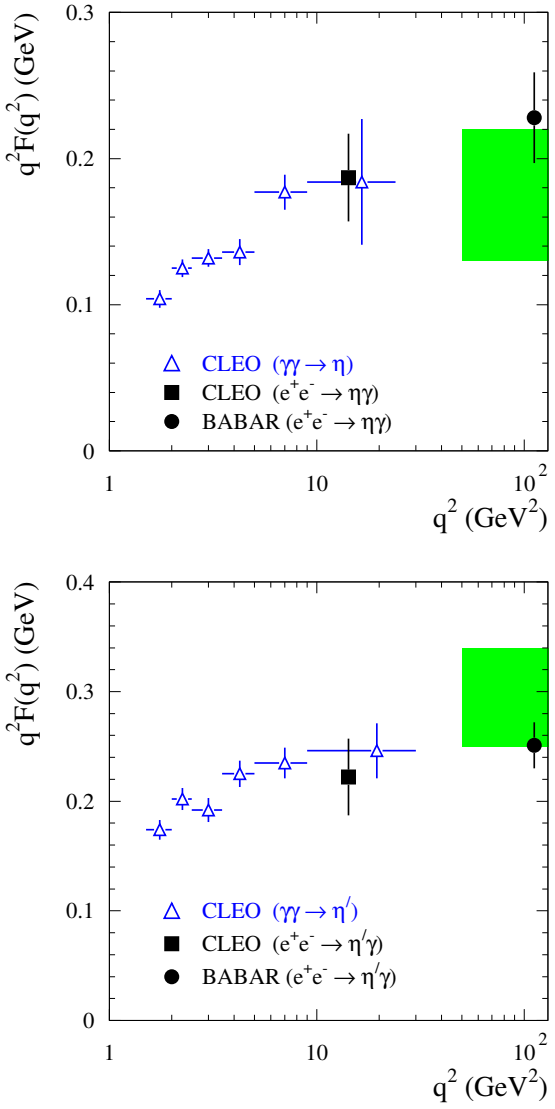

Fig. 5. The magnitudes of $\gamma\gamma^* \to \eta$ (top) and $\gamma\gamma^* \to \eta'$ (bottom) transition form factors multiplied by Q^2 measured by CLEO [3, 18] and BABAR [19]. The shaded boxes indicate the ranges of asymptotic form factor values calculated with the decay constants from Refs. [21–26].

Most precise high-Q^2 data obtained by the CLEO Collaboration [3] are shown in Fig. 5 (we averaged the CLEO results obtained in different η and η' decay modes).

The data on $e^+e^- \to \eta^{(\prime)}\gamma$ reactions also can be used to determine the transition form factors but in the time-like region $q^2 = s > 0$. Since the time- and space-like form factors are expected to be close at high Q^2, we show the results of high-Q^2 time-like measurements together with the CLEO space-like data. The form factors at $Q^2 = 14.2$ GeV^2 are obtained from the values of the $e^+e^- \to \eta^{(\prime)}\gamma$ cross sections measured by CLEO [18] near the maximum of the $\psi(3770)$ resonance. We use the natural assumption that the contributions of the $\psi(3770) \to \eta^{(\prime)}\gamma$ decays to the $e^+e^- \to \eta^{(\prime)}\gamma$ cross sections are negligible. It is seen that the measured time- and space-like form factors at $Q^2 \approx 14$ GeV^2 are close both for η and for η'. The time-like form factors at $Q^2 = 112$ GeV^2 were measured by BABAR [19].

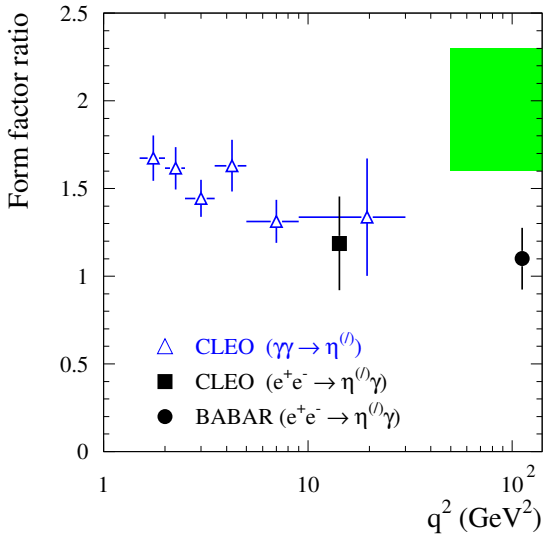

Fig. 6. The ratio of the $\gamma\gamma^* \to \eta'$ transition form factor to the $\gamma\gamma^* \to \eta$ form factor The shaded boxes indicate the range of predictions for the ratio of the asymptotic form factor factor.

The asymptotic limits for the η and η' form factors are calculated using Eq. (1) with the effective η and η' decay constants. The effective constants can be obtained, for example, in the flavor-mixing scheme [20]

$$f_\eta^{\rm eff} = (5f_{\rm n}\cos\phi - \sqrt{2}f_{\rm s}\sin\phi)/3, \quad (3)$$

$$f_{\eta'}^{\rm eff} = (5f_{\rm n}\sin\phi + \sqrt{2}f_{\rm s}\cos\phi)/3, \quad (4)$$

where $f_{\rm n}$ and $f_{\rm s}$ are the decay constants for the non-strange and strange components of η and η' mesons, and ϕ is the η- η' mixing angle. The values of the parameters $f_{\rm n}$, $f_{\rm s}$ and ϕ are determined from data, for example, on the radiative V to P transitions and the two-photon η and η' decays. Taking the results on the mixing parameters from Refs. [21–26] we obtain a range of predictions for the asymptotic limits. The asymptotic values were multiplied by the factor $(1 - 5/3 \cdot \alpha_{\rm s}(Q^2)/\pi)$ [27] to take into account next-to-leading perturbative QCD corrections at $Q^2 = 112$ GeV^2. The predictions are indicated by the shaded boxes in Fig. 5. The highest-Q^2 form factor data are at upper and lower ends of the range of predictions for η and η', respectively. It should be noted that the predictions for the η and η' effective decay constants are strongly correlated. In Fig. 6 we present the ratio of the η' form factor to the η form factor. The predicted ratio ranges from 1.6 to 2.3 and is inconsistent with the measured ratio at $Q^2 = 112$ GeV^2. This indicate that the η and η' distribution amplitudes have shapes strongly different from the asymptotic one.

4 Measurement of the $\gamma^*\gamma \to \eta_c$ transition form factor

The two-photon η_c production is studied both in no-tag and in single-tag modes. The η_c is reconstructed via its decay to $K_S K^- \pi^+$. The $KK\pi$ mass spectra for no-tag events is shown in Fig. 7.

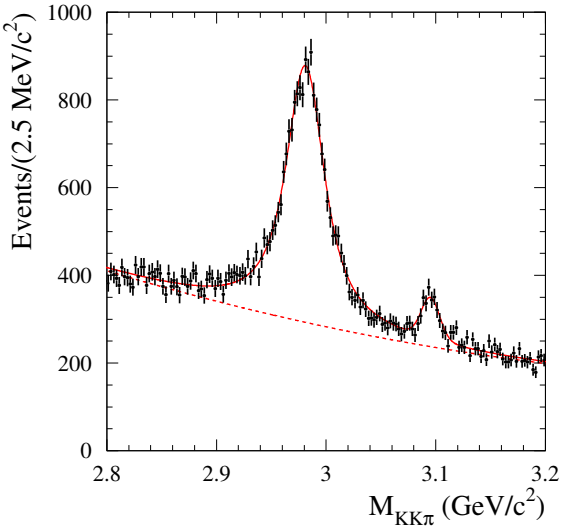

Fig. 7. The $K_S K^\pm \pi^\mp$ invariant mass distribution and fitted curve for no-tag data events.

The η_c and J/ψ peaks are clearly seen. The J/ψ's are produced in initial state radiation (ISR) process

$e^+e^- \to J/\psi\gamma$. From the fit to the mass spectrum we determine η_c parameters:

$$m = 2982.2 \pm 0.4 \pm 1.5 \text{ MeV}/c^2,$$

$$\Gamma = 31.7 \pm 1.2 \pm 0.8 \text{ MeV},$$

$$\Gamma(\eta_c \to \gamma\gamma)B(\eta_c \to K\bar{K}\pi) = 379 \pm 9 \pm 31 \text{ eV}.$$

These results are preliminary. Main sources of systematic uncertainties on the mass and width are unknown background shape and possible interference between η_c and non-resonant two-photon $K\bar{K}\pi$ amplitudes. The uncertainty on the detection efficiency dominates in the systematic uncertainty of $\Gamma(\eta_c \to \gamma\gamma)B(\eta_c \to K\bar{K}\pi)$. The results for the mass and width are in an agreement with the previous BABAR measurement [28]: $m = 2982.5 \pm 1.1 \pm 0.9$ MeV/c^2 and $\Gamma = 34.3 \pm 2.3 \pm 0.9$ MeV, obtained using 88 fb^{-1} data. The current PDG values for these parameters are $m = 2980.5 \pm 1.2$ MeV/c^2 and $\Gamma = 27.4 \pm 2.9$ MeV [29]. The obtained value of the product $\Gamma(\eta_c \to \gamma\gamma)B(\eta_c \to K\bar{K}\pi)$ agrees with the PDG value 0.44 ± 0.05 keV [29], and also with the recent CLEO measurement $0.407 \pm 0.022 \pm 0.028$ keV [30].

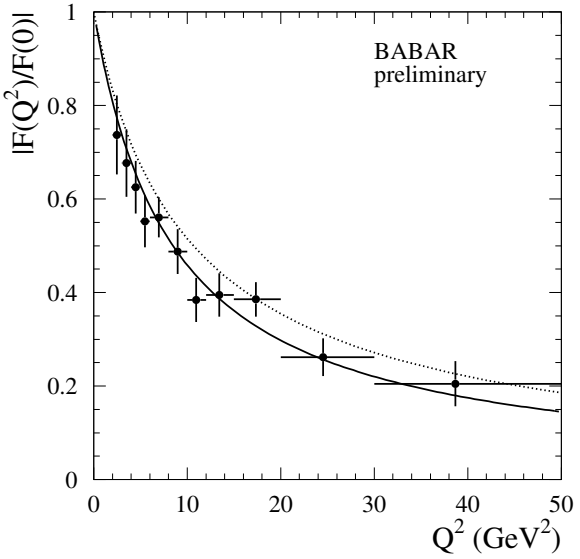

Fig. 8. The $\gamma\gamma^* \to \eta_c$ transition form factor normalized to $F(0)$ (points with error bars). The solid curve shows the interpolation given by a monopole form. The dotted curve shows the leading order pQCD prediction from Ref. [33].

We select $520 \pm 40 \pm 20$ single-tag η_c events. This number can be compared with 8 ± 5 events selected in the previous single-tag η_c measurement by L3 [31]. The single-tag data were divided into 11 Q^2 intervals. For each interval we fit to the $K\bar{K}\pi$ mass spectrum and determine number of events with η_c. From the ratio of the measured Q^2 spectrum to the number of the no-tag η_c events we extract the normalized η_c transition form factor shown in Fig. 8. The errors shown are combined statistical and Q^2-dependent systematic. There is also Q^2-independent error equal to 4.3%. Main source of the systematic error is the systematic uncertainty on detection efficiency.

The form factor data are fitted by the monopole function $|F(Q^2)/F(0)| = 1/(1 + Q^2/\Lambda)$. The result of the fit is shown in Fig. 8 by solid line. The pole parameter Λ is found to be $\Lambda = 8.5 \pm 0.6 \pm 0.7$ GeV^2. This value is in reasonable agreement with that expected from vector dominance, namely $\Lambda = m^2_{J/\psi} = 9.6$ GeV^2, and with the result of the lattice QCD calculation $\Lambda = 8.4 \pm 0.4$ GeV^2 [32]. The dotted curve in Fig. 8 shows results of the leading-order pQCD calculation of Ref. [33]. The data lie systematically below this prediction.

5 Summary

The $\gamma^*\gamma\pi^0$ transition form factor has been measured for Q^2 range from 4 to 40 GeV^2. The unexpected Q^2-dependence for the form factor is observed for $Q^2 > 10$ GeV^2. The data lie above the asymptotic limit. This indicates that the pion distribution amplitude should be wide. The measurement stimulated development of new models for the form-factor calculation, in particular, with flat distribution amplitude [12–14].

The data on $\gamma^*\gamma\eta$ and $\gamma^*\gamma\eta'$ transition form factors obtained by BABAR at $Q^2 = 112$ GeV^2 [18] indicate that the η and η' distribution amplitudes also strongly differ from the asymptotic DA.

The $\gamma^*\gamma\eta_c$ transition form factor has been measured for Q^2 range from 2 to 50 GeV^2. The form factor data are well described by the monopole form with pole parameter about 9 GeV^2. The data are in reasonable agreement with both QCD and VDM predictions.

References

1 Lepage G P, Brodsky S J. Phys. Rev. D, 1980, **22**: 2157
2 Aubert B et al (The BABAR collaboration). Phys. Rev. D, 2009, **80**: 052002
3 Gronberg J et al (CLEO collaboration). Phys. Rev. D, 1998, **57**: 33
4 Behrend H J et al (CELLO collaboration). Z. Phys. C, 1991, **49**: 401
5 Stefanis N G. Nucl. Phys. Proc. Suppl., 2008, **181-182**: 199
6 Bakulev A P, Mikhailov S V, Stefanis N G. Phys. Rev. D, 2003, **67**: 074012; Phys. Lett. B, 2004, **578**: 91
7 Lepage G P, Brodsky S J. Phys. Lett. B, 1979, **87**: 359
8 Chernyak V L, A. R. Zhitnitsky A R. Nucl. Phys. B, 1982, **201**: 492; B, 1983, **214**: 547
9 Bakulev A P, Mikhailov S V, Stefanis N G. Phys. Lett. B, 2001, **508**: 279 [Erratum-ibid. B, 2004, **590**: 309]
10 Mikhailov S V, Stefanis N G. Nucl. Phys. B, 2009, **821**: 291
11 Dorokhov A E. arXiv:0905.4577 [hep-ph]
12 Radyushkin A V. arXiv:0906.0323 [hep-ph]
13 Polyakov M V. JETP Lett., 2009, **90**: 228
14 LI H, Mishima S. Phys. Rev. D, 2009, **80**: 074024
15 Aihara H et al (TPC/Two Gamma collaboration). Phys. Rev. Lett., 1990, **64**: 172
16 Behrend H J et al (CELLO collaboration). Z. Phys. C, 1991, **49**: 401
17 Acciarri M et al (L3 collaboration). Phys. Lett. B, 1998, **418**: 399
18 Aubert B et al (BABAR collaboration). Phys. Rev. D, 2006, **74**: 012002
19 Pedlar T K et al (CLEO collaboration). Phys. Rev. D, 2009, **79**: 111101
20 Kroll P. Mod. Phys. Lett. A, 2005, **20**: 2667
21 Feldmann T, Kroll P, Stech B. Phys. Rev. D, 1998, **58**: 114006
22 Leutwyler H. Nucl. Phys. Proc. Suppl., 1998, **64**: 223
23 Benayoun M, DelBuono L, O'Connell H B. Eur. Phys. J. C, 2000, **17**: 593
24 Goity J L, Bernstein A M, Holstein B R. Phys. Rev. D, 2002, **66**: 076014
25 De Fazio F, M. R. Pennington M R. JHEP, 2000, **0007**: 051
26 Escribano R, Frere J M. JHEP, 2005, **0506**: 029
27 Braaten E. Phys. Rev. D, 1983, **28**: 524
28 Aubert B et al (BABAR collaboration). Phys. Rev. Lett., 2004, **92**: 142002
29 Particle Data Group, 2009 partial update for the 2010 edition, http://pdg.lbl.gov
30 Asner D M et al (CLEO collaboration). Phys. Rev. Lett., 2004, **92**: 142001
31 Acciarri M et al (L3 collaboration). Phys. Lett. B, 1999, **461**: 155
32 Dudek J J, Edwards R G. Phys. Rev. Lett., 2006, **97**: 172001
33 Feldmann T, Kroll P. Phys. Lett. B, 1997, **413**: 410